Supporting Online Material for

Functional Links Between Aβ Toxicity, Endocytic Trafficking and Alzheimer's Disease Risk Factors in Yeast

Sebastian Treusch, Shusei Hamamichi, Jessica L. Goodman, Kent E.S. Matlack, Chee Yeun Chung, Valeriya Baru, Joshua M. Shulman, Antonio Parrado, Brooke J. Bevis, Julie S. Valastyan, Haesun Han, Malin Lindhagen-Persson, Eric M. Reiman, Denis A. Evans, David A. Bennett, Anders Olofsson, Philip L. DeJager, Rudolph E. Tanzi, Kim A. Caldwell, Guy A. Caldwell and Susan Lindquist*

*To whom the correspondence should be addressed. E-mail: lindquist_admin@wi.mit.edu

This PDF file includes:

Materials and Methods

Yeast Experiments

Constructs, strains and growth conditions

The ssAβ 1-42 construct consists of attB sites for Gateway cloning the Kar2 signal sequence and the Aβ 1-42 sequence. The Aβ sequence was codon optimized for expression in yeast. The entire construct was synthesized and cloned into the Gateway entry vector pDONR221.

Sequence of the ssAβ construct: ACAAGTTTGTACAAAAAAGCAGGCTTCACAAA (Gateway flanking region)
ATGTTTTTCAACAGACTAAGCGCTGGCAAGCTGCTGGTACCACTCTCCGTGGTCCTGTAC
GCCCTTTTCGTGGTAATATTACCTTTACAGAATTCTTTCCACTCCTCCAATGTTTTAGTT
AGAGGT (Kar2 signal sequence)
GATGCTGAATTTAGACATGATTCTGGTTATGAAGTTCATCATCAAAAATTGGTTTTTTT
TGCTGAAGATGTTGGTTCTAATAAAGGTGCTATTATTGGTTTGATGGTTGGTGGTGTTG
TCATTGCTTAA (Aβ1-42)
ACCCAGCTTTCTTGTACAAAGTGGT (Gateway flanking region)

The same approach was used to generate the ssAβ 1-40 construct.

The BPTI WT and C51A constructs were the kind gift of Dane Wittrup (*21*). The original BPTI constructs do contain a signal sequence, but we replaced it with the Kar2 signal sequence (Kar2ss) in order to target them in the same manner as Aβ. The Kar2ss sequence and Gateway flanking regions were added to the BPTI ORFs using overlap extension PCR.

The Pdi1 gene is part of the overexpression library used in the screen. The Pdi1 gene was gateway cloned into the pDONR221 entry vector. The Aβ and BPTI constructs as well as Pdi1 were cloned into the pAG426Gal vector (*43*). Constructs were transformed into W303 Mat α, can1-100, his3-11,15, leu2-3,112, trp1-1, ura3-1, ade2-1 using a standard lithium acetate transformation protocol.

To generate ssAβ 1-42 screening strains the ssAβ 1-42 construct was moved to a pAG305Gal expression vector (*43*). The plasmid was digested using BstX1, gel purified and transformed into W303. The transformation was carried out in duplicate and the level of growth of 16 transformants each was tested on synthetic deficient media lacking leucine with galactose. Two strains from the independent transformations where selected as screening strains based on their robust yet intermediate toxicity that would allow for the identification of both suppressors and enhancers. Several transformants that showed no toxicity were selected as 1x ssAβ controls. The control strain for wild-type yeast growth is carrying a Gal-inducible YFP integrated in the same fashion as the ssAβ 1-42 constructs.

For spotting assays strains were grown over night at 30°C in 3 mL SD media lacking the relevant amino acids and containing glucose. Cell concentrations (OD_{600})

were adjusted in a 96-well plate to that of the strain with the lowest concentration. Cells were then 5-fold serially diluted and spotted on SD media containing glucose (Uninduced) and galactose (Induced). Plates were incubated at 30°C for 2 (glucose) or 3 days (galactose).

Propidium Iodide staining

For the Propidium Iodide (PI) staining of dead yeast cells, strains were pre-grown in raffinose media over night and then induced in galactose media for 16 hr (5 mL OD_{600} 0.5). Cells were incubated with 20 μg/mL PI for 15 min, washed with PBS and then cells positive for red PI staining were counted on a flow cytometer (Guava System). 5000 cells for each sample were counted and the percent of cells that stained positive for PI were recorded. Control dead cells were generated by incubating a culture at 100°C for 5 min.

Cell lysis

Strains were grown in synthetic deficient media lacking leucine and uracil (SD-Leu-Ura) with raffinose overnight at 30°C. Cultures were the diluted into inducing media containing galactose (OD_{600} 0.2) and grown for 8h. Cells were spun down for 5min at 3,000rpm. For preparation of yeast lysates, yeast pellets were resuspended in 200 μL of yeast lysis buffer (50mM HEPES pH 7.5, 150mM NaCl, 2.5mM EDTA, 1% v/v Triton-X 100 with protease inhibitors). To this solution, 200 μL of glass beads (Aldrich) were added, and the yeast were bead beaten for 3 minutes on maximum speed at 4°C. Afterwards, the sample was retrieved by puncturing a hole in the bottom of the eppendorf tube and spinning the samples into a new tube at 6,000 rpm for 15 seconds. The supernatant was transferred to a new tube, and this solution was used as the lysate.

Western blot protocol

For the western blot, the protein concentrations in the yeast lysates were normalized using the results from a BCA assay (Pierce). After normalization, samples were loaded on a 4-12% Bis-Tris gel (Invitrogen) and run at 150 V for approximately 50 minutes. Subsequently, the samples were transferred to 0.2 micron PVDF membrane (Bio-Rad). After the transfer was completed, the membrane was blocked with 5% milk in PBS overnight. The membrane was briefly washed with PBS before the primary antibody, 6E10 (Covance) was added at a 1:1,000 dilution in 5% milk in PBS. The primary antibody was allowed to incubate for 2.5 hrs, after which the blot was washed 4 x 5 minutes with PBS. The anti-mouse secondary (DyLight, Rockland) was added at a 1:10,000 dilution in 5% milk in PBS for 1 hr. The blot was washed 4 x 5 minutes with PBS. The blot was scanned using the Licor Odyssey Scanner.

For detection of oligomers using the NAB61 antibody, the antibody was diluted 1:500 in 5% milk in PBS and incubated with the blot. Subsequently, the blot was washed 4 x 5 minutes with PBS. The anti-mouse secondary (DyLight, Rockland) was

added at a 1:10,000 dilution in 5% milk in PBS for 1 hr. The blot was washed 4 x 5 min with PBS. The blot was scanned using the Licor Odyssey Scanner.

Indirect ELISA protocol

The indirect ELISA using the OMAB oligomer specific antibody was performed as described in Lindhagen-Persson *et al*. (*22*). Briefly, the oligomer specific monoclonal OMAB antibody (Agrisera AB, Vännäs, Sweden) was diluted to a concentration corresponding to 5 μg/mL and was coated to a 96-well polystyrene microtiterplate (F96 Nunc immunosorp, Denmark) overnight. Unspecific sites were blocked using 5% dry milk dissolved in PBS. Frozen yeast lysates were thawed on ice and centrifuged at 20,000 x g for 5 minutes followed by 3 serial dilutions in PBS. The plate that was coated with the OMAB antibody was washed with water and 100 μl of the samples was applied in 5 replicates. The samples were incubated at room temperature for 25 minutes, and the plate was subsequently washed 4 times with PBS containing 0.15% Tween-20. Bound Aβ was detected using a polyclonal rabbit anti-Aβ antibody (antibody AS08 357, Agrisera AB, Vännäs Umeå) that was dissolved in blocking buffer at a 1:2,000 dilution. The rabbit antibody was allowed to incubate for 30 minutes, after which the plate was washed with PBS containing 0.15% Tween-20. A secondary anti-rabbit IgG-HRP (GE-healthcare, Buckinghamshar, UK) dissolved in blocking buffer was used to detect bound rabbit IgG. Before addition of the detection reagent, excess secondary anti-rabbit IgG-HRP was removed by washing with PBS containing 0.15% Tween-20. The plate was developed using 100 μL EC-blue® (Medicago, Uppsala, Sweden). Measurements were made at 400 nm and 600 nm, and the absorption ratio between 600 nm and 400 nm was used to calculate the amount of binding. Statistical significance was determined using the paired *t*-test. For the lysate plus monomeric Aβ sample, monomeric Aβ was added to vector control cells that were being lysed. These samples were analyzed in the OMAB ELISA assay. No signal was detected in the lysate samples spiked with monomeric Aβ peptide, supporting that the assay does not detect monomeric Aβ, and that our lysis conditions do not induce Aβ oligomerization.

Size exclusion chromatography was used to analyze the relative sizes of oligomers formed in our yeast ssAβ 1-42 screening strains. Lysates of the ssAβ 1-42 screening strains were separated on a superose-12 HR column 20 mL PBS. Fractions were collected and each fraction was analyzed in triplicate using the OMAB antibody in an indirect ELISA assay. To determine the molecular weight of each fraction, a standard of known proteins (BioRad 151-1901) was used as well as a single run of monomeric Aβ 1-42. Under these chromatography conditions, monomeric Aβ 1-42 migrates with an apparent molecular weight of about 11 kDa. Dimers and tetramers also have this 11 kDa exclusion volume. When the size of the Aβ oligomers increase (larger than tetramers), the "non-ideal behavior" of Aβ diminishes and Aβ behaves as a normal globular protein.

Immunostaining

Strains were pre-grown in raffinose media overnight and then induced in galactose media for 16 hr (5 mL OD_{600} 0.5). Cells were spun down and resuspended in 5 mL of 4% formaldehyde, 50mM KP_i, pH 7.4, 1mM $MgCl_2$. Cells were fixed for 2 hrs. After fixation, cells were washed 3 times in 5 mL of wash buffer (0.1M KP_i pH 7.4, 1mM $MgCl_2$, Complete Mini Protease Inhibitors (Roche)) and then resuspended to a final OD_{600} of 10 in the wash buffer. 100 μL of cells were incubated with 0.6 μL of 2-mercaptoethanol and 20 μL of yeast lytic enzyme (25,000U/mL; ICN) for 10min and then washed and gently resuspended in 100 μL wash buffer. Ten μL of the spheroplast suspension was added to a polylysine-coated coverglass, incubated for 3 min and then blotted dry. The dried coverglass was submerged in 40 mL of acetone precooled to -20°C in a 50-mL Falcon tube. After 5 min, the coverglass was removed, inverted onto a paper towel and allowed to dry. Each well was pre-coated for 30 min with PBS-Block (PBS, pH7.4, 1% dried milk, 0.1% bovine serum albumin, 0.1% octyl glucoside). Block was gently removed by aspirating and 10 μL of the primary antibody mixture (PBS-Block, 1:200 6E10 Aβ antibody) was added. Following a 1-hr incubation, the primary antibody was gently washed off 8 times with PBS-Block. Ten μL of the secondary antibody mixture (PBS-Block, 1:100 anti-mouse FITC, 2 μg/mL Hoechst 33258) was added, incubated for 30min in the dark and washed off 8 times. The liquid was aspirated completely after the final wash. 5 μL of mounting medium was added to each well before it was placed on a slide and sealed with nail polish.

Images were taken on a Nikon Eclipse Ti inverted microscope using a Roper Scientific CoolSNAP HQ camera. Z-stacks were taken at a distance of 0.3 μM between slices and the NIS Elements Microscope Imaging Software was used to deconvolve and process the images.

Sample preparation for mass spectrometry

Control and ssAβ 1-42 strains were induced, lysed and subsequently immuno-precipitated with the 6E10 antibody. The immuno-precipitated material was subjected to SDS-PAGE and silver staining. The ~3.5 kDa and 6 kDa region of the control and ssAβ screening strain lanes were excised. These bands of interest were divided into ~2 mm squares and washed overnight in 50% methanol/ water. These were washed once more with 47.5/47.5/5% methanol/water/acetic acid for 2 hrs, dehydrated with acetonitrile and dried in a speed-vac. Reduction and alkylation of disulfide bonds was then carried out by the addition of 30 μL of 10mM dithiothreitol (DTT) in 100mM ammonium bicarbonate for 30 min to reduce disulfide bonds. The resulting free cysteine residues were subjected to an alkylation reaction by removal of the DTT solution and the addition of 100mM iodoacetamide in 100 mM ammonium bicarbonate for 30 min to form carbamidomethyl cysteine. These were then washed with aliquots of acetonitrile, 100mM ammonium bicarbonate and acetonitrile and dried in a speed-vac. The bands were enzymatically digested by the addition of 300 ng of trypsin in 50mM ammonium bicarbonate to the dried gel pieces ratio of mg trypsin for 10 min on ice. Depending on the volume of acrylamide,

excess ammonium bicarbonate was removed or enough was added rehydrate the gel pieces. These were allowed to digest overnight at 37°C. The resulting peptides were extracted by the addition of 50 μL (or more if needed to produce supernatant) of 50mM ammonium bicarbonate with gentle shaking for 10 min. The supernatant from this was collected in a 0.5 mL conical autosampler vial. Two subsequent additions of 47.5/47/5/5 acetonitrile/water/formic acid with gentle shaking for 10 min were performed with the supernatant added to the 0.5 mL autosampler vial. Organic solvent was removed and the volumes were reduced by to 15 μL using a speed vac for subsequent analyses.

Chromatographic separations

Digestion extracts were analyzed by reversed phase high performance liquid chromatography (HPLC) using a Waters NanoAcquity HPLC and autosampler and a ThermoFisher LTQ linear ion trap mass spectrometer using a nano flow configuration. A 20 mm x 180 micron column packed with 5 micron Symmetry C18 material (Waters) using a flow rate of 15 μL per minute for two minutes was used to trap and wash peptides. These were then eluted onto the analytical column which was a self-packed with 3 micron Jupiter C18 material (Phenomenex) in a fritted 10 cm x 75 micron fused silica tubing pulled to a 5 micron tip. The gradient was isocratic 1% A Buffer for 1 min 250 nL min-1 with increasing B buffer concentrations to 40% B at 20 min. The column was washed with high-percent B and re-equlibrated between analytical runs for a total cycle time of approximately 37 min. Buffer A consisted of 1% formic acid in water and buffer B consisted of 1% formic acid in acetonitrile. (Alternatively, a linear gradient of 1% to 40% B from time 1 min to time 24.5 min is used as an alternative for very low level samples where staining indicates a single band.)

Mass spectrometry of isolated proteins

The ThermoFisher LTQ linear ion trap mass spectrometer was operated in a dependant data acquisition mode where the five most abundant peptides detected in full scan mode were subjected to daughter ion fragmentation. A running list of parent ions was tabulated as an exclusion list to increase the number of peptides analyzed throughout the chromatographic run.

Mass spectrometry data analysis

Peptides were identified from the MS data using SEQUEST algorithms that searched a species-specific database generated from NCBI's non-redundant (nr.fasta) database. Sequest filters used for indication of a positive peptide identification were: XCorr vs. Charge State = 1.5, 2.00, 2.50; Sp – Preliminary Score = 500. Two peptides were required for a protein to be considered a positive identification. Data interpretation from all bands was aided by the MSRAT program (Protein Forest) or Scaffold (Proteome Software).

Halo secretion assay

The α-syn control strain used in this assay was Mata, 303 Gal α-syn YFP, 304 Gal α-syn YFP, leu2-3,112 trp1-1 can1-100 ura3-1 ade2-1 his3-11,15. Tested strains were struck onto a YPD plate (w/v – 1% yeast extract, 2% peptone, 2% glucose, adjusted to pH 7.0, 2% agar) and grown overnight at 30°C. The next day bar1 cells were grown for 4 hrs in YPD (w/v – 1% yeast extract, 2% peptone, 2% glucose, adjusted to pH 7.0) before being diluted 1:50 and plated as a lawn on both YPD and YPGal (w/v – 1% yeast extract, 2% peptone, 2% glucose, adjusted to pH 7.0, 2% agar) plates. After the lawns dried, the strains to test were scrapped from the plate and diluted into sterile water. For uninduced controls, 10 μL of culture diluted to an OD_{600}=1.0 was spotted in the center of the YPD plate. For the inducing YPGal plates, an OD_{600}=1.0 was used for α-syn and the toxic Aβ screening strain 1, while an OD_{600}=0.04 was used for the vector control strain to account for the difference in rate of growth. Pictures were taken after two days of growth at 30°C.

Screen for modifiers of Aβ toxicity

The overexpression library screened contains ~5800 full-length sequence verified yeast ORFs in the galactose-inducible Gateway expression plasmid pBY011 (*CEN*, *URA3*, AmpR) (*2*). The library is arrayed in 96-well format. Plasmid DNA was prepared by pin inoculation into deep well 96-well plates containing 1.8mL LB-AMP, growth over night at 37°C and 96-well mini preps using a Qiagen BioRobot 8000. The DNA was transformed into a ssAβ screening strain (ssAβ1-42 p305) carrying a Gal4-ER-VP16 plasmid (*CEN*, *HIS3*, AmpR), which allows for expression from GAL promoters on carbon sources other than galactose in the presence of estradiol in the yeast media (*44*). Neither estradiol nor the Gal4-ER-VP16 plasmid had an effect on Aβ toxicity on its own. Transformations were carried out using a standard lithium acetate transformation protocol adapted for a 96-well format and automation using a Tecan Evo 150 liquid handling robot. Transformants were grown in synthetic deficient media lacking histidine, leucine, and uracil (SD-His-Leu-Ura) with glucose overnight. The cells were then diluted in water and spotted on SD-His-Leu-Ura agar plates containing glucose alone (control), galactose alone, glucose plus 1μM estradiol (Sigma E1024) or glycerol plus 1μM estradiol using a Singer RoToR pinning robot and long 96-well pins. Putative enhancers and suppressors were identified after 2-4 days of growth at 30°C. Putative screen hits were cherry picked from the plasmid library, retransformed into two independent derived ssAβ screening strains and retested on the three screening conditions in two independently derived strains. We eliminated hits that have known effects on GAL induction and genes whose overexpression has previously been shown to be toxic. To further exclude false-positive suppressors we used flow cytometry to measure the expression of YFP in their presence. To further exclude false-positive enhancers that cause a general inhibition when overexpressed we examined their effects in the YFP control strain, which has no growth impairment. The identity of confirmed modifiers was verified by sequencing.

Flow cytometry

A strain carrying an integrated YFP was transformed with the putative Aβ suppressors. The resulting strains were grown in glucose media in a 96-well format, diluted into the various inducing media (galactose, glucose +1μM estradiol, glycerol + 1μM estradiol) [5 μL culture added to 120 μL media], and incubated over night at 30°C with mild shaking. These overnight cultures were diluted 20-fold into water and YFP levels were measured using a Guava flow cytometer. Each strain was measured 3 times and 5000 cells were counted for each well. The whole experiment was repeated 3 times. Values are averages of these 3 experiments and reported in percent of the vector control strain YFP levels.

Microscopy of Clc1-GFP and Ste3-YFP

We created our own version of the Ste3 localization assay (*38*) by generating a *GPD*-driven Ste3-YFP construct, using the Ste3 plasmid from our ORF library and a *GPD* p303 vector from the pAG collection (*43*), and integrating it into an ssAβ 1-42 screening strain as well as a control strain. We tested the effect of selected modifiers by transforming these strains with the modifiers and analyzing them in the same fashion. Ste3-YFP normally localizes to the vacuole, typically a single large, round spot in normal cells. In cells expressing Aβ, the normal vacuolar pattern is gone after induction with galactose; the Ste3-YFP intensity is dimmer, probably due to incorrect trafficking, and appears in smaller, irregularly shaped intracellular structures. The co-expression of the Aβ modifiers reversed this phenotype. For all microscopy experiments strain were pre-cultured in raffinose media and then induced in galactose media for 16 hr. Images were taken on a Nikon Eclipse Ti inverted microscope using a Roper Scientific CoolSNAP HQ camera. Z-stacks were taken at a distance of 0.3 μM between slices and the NIS Elements Microscope Imaging Software was used to deconvolve and process the images. The intensity of the control Ste3-YFP strain was significantly brighter than the cells expressing Aβ, so we had to increase the exposure time in order to see an interpretable signal. The control strain was imaged for 230ms, while the Aβ-expressing strains were all exposed for 1.15s. Aside from the difference in exposure time, we processed all of the samples exactly the same. Aβ expression for the indicated time resulted in a size decrease of yeast vacuoles, likely due to the decrease in trafficking to them, but otherwise did not alter their morphology.

To examine the effects of Aβ on endocytosis, we mated the Aβ screening strains to the clathrin light chain (Clc1)-GFP strain from the GFP library (*46*). The Clc1-GFP fluorescence pattern in normal cells is 4 - 8 foci, scattered throughout the cell. Upon induction of Aβ, the number of the foci was increased, while the size of the foci decreased. We also used GFP-fusion strain of other endocytic proteins (Abp1, Sla1 and Sla2) and observed similar Aβ-induced changes in localization as with Clc1-GFP (data not shown); yet the fluorescence of these fusions was rather low. Images were captured and processed as described above.

C. elegans Experiments

Plasmid & Constructs

The following cDNAs were cloned into pDONR221 using Gateway Technology (Invitrogen, San Diego, CA): *ssAβ 1-42* (Chris Link, University of Colorado, for the signal sequence we used Chris Link's *C. elegans* signal sequence: ATGCATAAGGTTTTGCTGGCACTGTTCTTTATCTTTCTGGCACCAGCAGGTACC); *gfp* and *lacZ* (Andy Fire, Stanford University); *mCherry*; *C13G3.3*, *C32E8.10*, and *C37H5.6* (Worm ORFeome collection from Marc Vidal) (*47*); *XPO1* (human ORFeome collection from Marc Vidal) (*48*); and *JC8.10*, *Y44E3A.4*, and *F42G10.2*. *JC8.10*, *Y44E3A.4*, and *F42G10.2* were isolated from our *C. elegans* cDNA library. The cDNAs were verified by DNA sequencing, and subsequently cloned into pDEST-EAT-4. pDEST-EAT-4 was generated by PCR amplification of a *eat-4* promoter, double digestion of the promoter and pDEST-UNC-54 using *BplI* and *KpnI*, and replacement of a *unc-54* promoter in pDEST-UNC-54 with a *eat-4* promoter via ligation reaction.

Nematode Strains

Nematodes were maintained following standard procedures (*49*). To make a worm ssAβ 1-42 model UA162 [*baEx*107; P*eat-4*::ssAβ 1-42, P*eat-4*::gfp, P*myo-2*::mCherry], 50 μg/mL of P*eat-4*::ssAβ 1-42 and P*eat-4*::gfp as well as 2.5 μg/mL of P*myo-2*::mCherry were injected into wild-type N2 (Bristol) worms. This strain was integrated by using Spectrolinker XL-1500 (Spectronics Corporation, Westbury, NY) and outcrossed three times to N2 worms to generate UA166 [*baInl*32; P*eat-4*::ssAβ 1-42, P*eat-4*::gfp, P*myo-2*::mCherry]. For neuroprotection analysis, three stable lines of UA163 [*baEx*108; [P*eat-4*::C13G3.3, rol-6 (su1006)], UA164 [*baEx*109; [P*eat-4*::C32E8.10, rol-6 (su1006)], and UA165 [*baEx*110; [P*eat-4*::C37H5.6, rol-6 (su1006)] were made and crossed with UA166 [*baInl*32; P*eat-4*::ssAβ 1-42, P*eat-4*::gfp, P*myo-2*::mCherry] to generate UA167 {[*baInl*32; P*eat-4*::ssAβ 1-42, P*eat-4*::gfp, P*myo-2*::mCherry]; *baEx*108; [P*eat-4*::C13G3.3, rol-6 (su1006)]}, UA168 {[*baInl*32; P*eat-4*::ssAβ 1-42, P*eat-4*::gfp, P*myo-2*::mCherry]; *baEx*109; [P*eat-4*::C32E8.10, rol-6 (su1006)]}, and UA169 {[*baInl*32; P*eat-4*::ssAβ 1-42, P*eat-4*::gfp, P*myo-2*::mCherry]; *baEx*110; [P*eat-4*::C37H5.6, rol-6 (su1006)]}. Furthermore, three stable lines of UA170 {[*baInl*32; P*eat-4*::ssAβ 1-42, P*eat-4*::gfp, P*myo-2*::mCherry]; *baEx*111; [P*eat-4*::JC8.10, rol-6 (su1006)]}, UA171 {[*baInl*32; P*eat-4*::ssAβ 1-42, P*eat-4*::gfp, P*myo-2*::mCherry]; *baEx*112; [P*eat-4*::Y44E3A.4, rol-6 (su1006)]}, UA172 {[*baInl*32; P*eat-4*::ssAβ 1-42, P*eat-4*::gfp, P*myo-2*::mCherry]; *baEx*113; [P*eat-4*::XPO1, rol-6 (su1006)]}, UA173 {[*baInl*32; P*eat-4*::ssAβ 1-42, P*eat-4*::gfp, P*myo-2*::mCherry]; *baEx*114; [P*eat-4*::F42G10.2, rol-6 (su1006)]}, UA174 {[*baInl*32; P*eat-4*::ssAβ 1-42, P*eat-4*::gfp, P*myo-2*::mCherry]; *baEx*115; [P*eat-4*::mCherry, rol-6 (su1006)]}, and UA175 {[*baInl*32; P*eat-4*::ssAβ 1-42, P*eat-4*::gfp, P*myo-2*::mCherry]; *baEx*116; [P*eat-4*::lacZ, rol-6 (su1006)]} were generated by directly injecting 50 μg/mL of putative ssAβ 1-42 toxicity modifiers and *rol-6* into UA166 [*baInl*32; P*eat-4*::ssAβ 1-42, P*eat-4*::gfp, P*myo-2*::mCherry].

Neuroprotection Analysis

For analysis of putative ssAβ 1-42 toxicity modifiers, the transgenic worms were age-synchronized (*50*), transferred onto NGM plates, and grown at 20°C for 3 or 7 days. For each trial, 30 worms were transferred to a 2% agarose pad, immobilized with 2mM levamisole, and scored. Worms were considered rescued when all five posterior glutamatergic neurons were intact and had no visible signs of degeneration. Each stable line was analyzed three times (for a total of 90 worms/transgenic line). Three separate transgenic lines were analyzed per gene (for a total of 270 animals/gene). Imaging and statistics were performed as described previously (*51*).

Semi-quantitative RT-PCR

RNA isolation and semi-quantitative RT-PCR were performed as described previously (*51*). Briefly, total RNAs were isolated from 50 L3-staged worms, amplified using SuperScript III RT (Invitrogen) with oligo dT primers, and treated with amplification grade RNase-free DNase I (Invitrogen) as well as RNase H (Invitrogen) following the manufacture's protocol. The following primers were designed for the PCR:

cdk-5	Primer 1:	5' ggg-gat-gat-gag-ggt-gtt-cca-agc 3'
	Primer 2:	5' ggc-gac-cgg-cat-ttg-aga-tct-ctg-c 3'

The trangenes were PCR amplified by using primer sequences specific to *unc-54* 3'UTR and each respective open reading frame.

unc-54 3'UTR	Primer 1:	5' gac-tta-gaa-gtc-aga-ggc-acg-ggc 3'
ssAβ 1-42	Primer 2:	5' atg-cat-aag-gtt-ttg-ctg-gca-ctg-ttc-ttt-atc 3'
C13G3.3	Primer 2:	5' gag-aaa-cag-gca-atg-gga-aac-ccg-c 3'
C32E8.10	Primer 2:	5' gct-gct-cca-ttc-gga-tat-cca-aat-gc 3'
C37H5.6	Primer 2:	5' gga-gta-acg-act-gga-cgt-aaa-cgt-cg 3'
JC8.10	Primer 2:	5' gat-cga-cct-cgt-cca-cca-tca-gc 3'
Y44E3A.4	Primer 2:	5' cac-tga-tca-ggt-cgc-cga-act-gc 3'
F42G10.2	Primer 2:	5' cat-gac-gcc-ggt-tgt-cag-ccg 3'
XPO1	Primer 2:	5' gtg-aca-gac-act-tca-cat-act-gct-gg 3'
mCherry	Primer 2:	5' gat-gaa-ctt-cga-gga-cgg-cgg-c 3'
lacZ	Primer 2:	5' gcc-tta-ctg-ccg-cct-gtt-ttg-acc 3'

Cortical Neuron Experiments

Soluble Aβ oligomer and Aβ fiber preparations

Soluble oligomers were prepared as in Kayed *et al. (13)*. In brief, lyophilized Aβ 1-42 (American Peptide Company) was resuspended in 200 μL of HFIP (1,1,1,3,3,3-Hexafluoro-2-propanol, Aldrich), and this solution was bath sonicated for 30 min. Subsequently, 100 μL of the HFIP solution was added to 900 μL of ddH2O in a siliconized eppendorf tube. This solution was incubated at room

temperature for 10-20 min. After the room temperature incubation, the HFIP in the sample was evaporated using a gentle stream of N_2 for approximately 20 min. The samples were allowed to incubate at room temperature for 48 hrs, after which they were frozen and stored at -80°C. Oligomers were characterized by SDS-PAGE analysis as described above and by SDD-AGE as described in Halfmann and Lindquist (*45*). Fibers were prepared by dissolving 0.5 mg of Aβ 1-42 (American Peptide Company) in 200 μL HFIP. The resulting solution was bath sonicated for 30 min at room temperature. The resulting disaggregated Aβ sample was dried to a peptide film using a gentle stream of N_2. Subsequently, the peptide film was resuspended in 93.75 μL of DMSO, and to this solution, 1300 μL of 10mM HCl was added. The samples were incubated at 37°C for several days without shaking. Fibers were characterized using SDD-AGE. Electron Microscopy was performed at the W.M. Keck Microscopy Facility at the Whitehead Institute. For preparation of the EM samples, the fibers were adhered to a copper surface and stained with 2% uranyl acetate. The fibers were imaged using a FEI Technai Spirit Transmission Electron Microscope.

Rat primary cortical cultures

Cultures were prepared based on Lesuisse and Martin (*52*). Embryos were harvested by cesarean section from anesthetized pregnant Sprague-Dawley rats at embryonic day 18. Cerebral cortices were isolated and dissociated with Accumax digestion for 20 min at 37°C and trituration with Pasteur pipette. Poly-ornithine and laminin-coated 96-well plates were seeded with $4x10^4$ cells in Neurobasal medium (Life Technologies) supplemented with B27 (Life Technologies), 0.5mM glutamine, 25μM β–mercaptoethanol, penicillin (100 IU/mL) and streptomycin (100 μg/mL). One third of the medium was changed every 3 to 4 days. Aβ oligomer (final concentration 750nM) or vehicle was added to the lentivirus-transduced cultures in 96-well plates at DIV 18. As a surrogate marker of cell viability, cellular ATP content was measured after 20 hrs of Aβ oligomer incubation using ViaLight Plus kit (Lonza). As a secondary method for quantitating neuronal toxicity, neurons were stained with an antibody specific for the neuronal marker MAP2 (see details below).

Lentivirus production and transduction to rat primary cortical cultures

pLENTI6/V5 DEST (Invitrogen) lentivirus expression vector was used to generate lentivirus encoding *GFP*, *PICALM* and *RAB1*. Lentiviral constructs were packaged into virus via lipid-mediated transient transfection of the expression constructs and packaging plasmids (pMD2.G and psPAX2) to 293 cells. Lentivirus was purified and concentrated using Lenti-X Maxi Purification kit and LentiX Concentrator (Clontech) according to the manufacturer's protocol. Lentivirus titer was determined using QuickTiter Lentivirus titer kit (Lentivirus- Associated HIV p24; Cell Biolabs) according to the manufacturer's protocol. Rat cortical cultures were transduced with various multiplicities of infection (MOI) of lentivirus at DIV 5.

Immunocytochemistry and quantification of viable neurons.

For imaging, cells were cultured in PerkinElmer View plates-96F TC (Waltham, MA), coated with poly-ornithine / laminin. For immunohistochemical staining, cells were rinsed with PBS, fixed in 4% paraformaldehyde for 20 min, permeabilized and blocked for 1 hr in blocking buffer (PBS, containing 0.1% Triton X100 and10% normal donkey serum). Cells were then incubated with rabbit polyclonal antibodies against MAP2 (1:500, Millipore, Temecula, CA) in blocking buffer at 4°C overnight. After the primary antibody incubation, cells were rinsed with PBS and incubated with secondary antibodies (Alexa Fluor 568 donkey anti-rabbit IgG (1:500, Invitrogen) for 1 hr at room temperature. Subsequently, the neurons were rinsed three times with PBS, and nuclei were stained with Hoechst 33342 (Invitrogen) for 15 min and rinsed with PBS. Images were taken using an Eclipse Ti Nikon microscope (10x objective). The number of live neurons was determined by manually counting MAP2 and Hoechst-positive cells from random 20 fields per well, 3 wells per condition.

Analysis of ROS and MAP data sets

We leveraged available genotyping, and extensive clinical and pathological data from two large epidemiological studies of aging, cognition, and AD: the Religious Orders Study (ROS) and the Rush Memory and Aging Project (MAP). These studies enlisted more than 2,300 older persons, without dementia at baseline, who were clinically evaluated annually and who agreed to brain donation upon death. Nearly 900 autopsies have been completed. Recent studies in these cohorts demonstrate how intermediate AD-related cognitive and pathological phenotypes can enhance power for genetic association analysis (*33, 34, 53*). For our study, we utilized a combined cohort of 1,593 ROS and MAP subjects with longitudinal neuropsychiatric assessments and genome-wide genotyping, and a nested pathological cohort including 651 brain autopsies (Table S4).

We initially determined whether the modifiers correspond to loci that impact susceptibility for episodic memory decline, a cardinal feature of AD. In ROS and MAP, rate-of-change in memory performance is characterized based on repeated assessment of 7 neuropsychiatric tests, and our analyses were additionally adjusted for age, gender and years of education. We implemented a locus-based association test for memory decline, considering all common single nucleotide polymorphisms (SNPs) at each candidate locus, including both directly genotyped and imputed variants, based on the HapMap reference (*54*) (Table S5 & S6). We tested if the observed associations were significant, by performing a permutation procedure to compute an empirical *P*-value (P_{perm}), adjusting for the multiple tests performed at each locus. Aside from *PICALM* (*rs7128598*, *P*-value=$1.6\text{x}10^{-4}$, P_{perm}=0.012), several other loci harbored SNPs suggesting association with memory decline, but these results did not remain significant following permutation (Table S6).

We investigated whether our modifiers are associated with the development of AD neuropathology. These analyses used a quantitative summary measure of global AD pathologic burden, based on counts of amyloid plaques and NFTs on brain tissue sections. The relations of SNPs with this continuous measure of pathology were

tested using linear regression, adjusting for age at the time of death. Notably, these analyses indicate association of 2 additional loci identified by our yeast screen, *ADSSL1* (*rs1128880*, *P*=0.001, P_{perm} =0.031) and *RABGEF1* (*rs17566701*, *P*=0.002, P_{perm} =0.038) with AD neuropathology (Table S7). Both of these loci also harbored suggestive association signals with episodic memory decline in the larger clinical cohort, showing a statistical trend toward significance following the permutation procedure (Table S6).

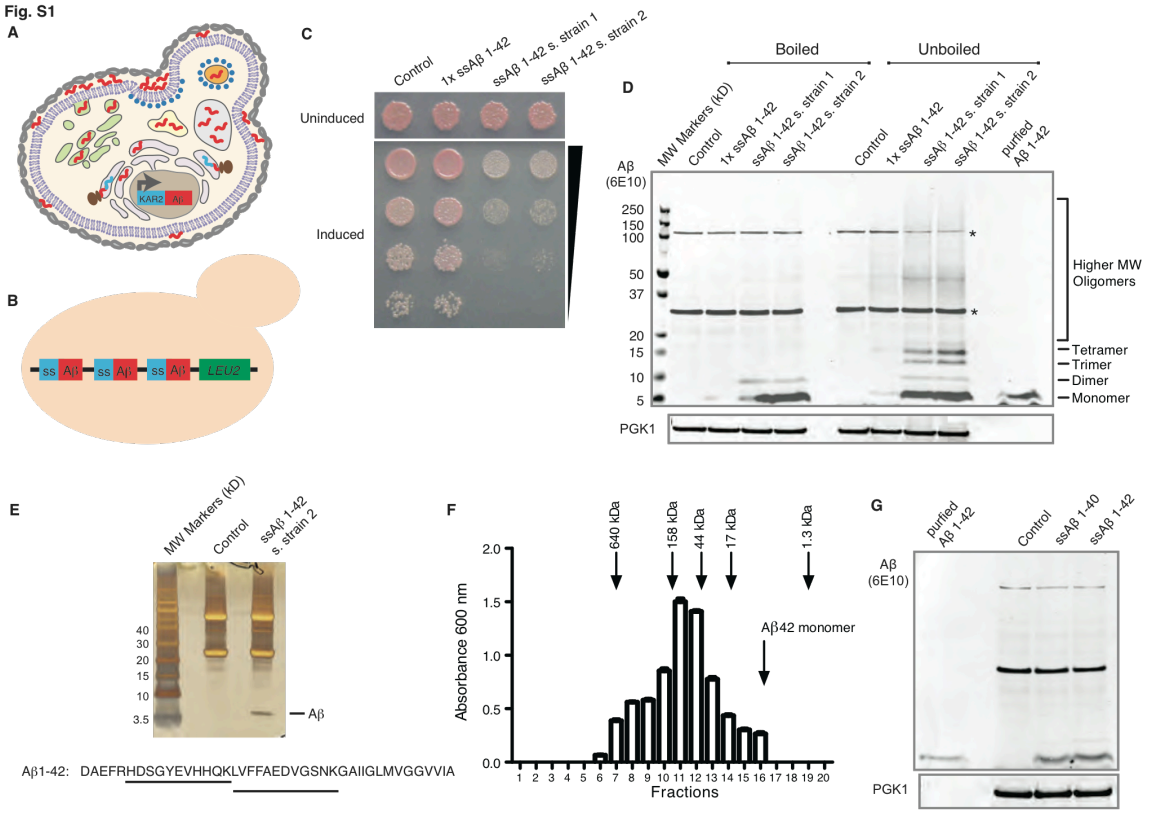

Fig. S1. Characterization of strains expressing Aβ

(A) The ssAβ 1-42 construct is a fusion of the KAR2 signal sequence to the N-terminus of the Aβ 1-42 sequence. The signal sequence is cleaved in the ER, releasing Aβ 1-42 into the secretory pathway. Yeast organelles represented include: ER (light purple), Golgi network (green), endocytic vesicles (orange), recycling endosomes (yellow) and the vacuole (white), blue circles represent clathrin, ribosomes are brown. (B) The genetic screening strains were generated by integrating multiple tandem copies of the ssAβ 1-42 construct into the LEU2 locus of W303 strains (see Materials and Methods). (C) Construction of two independent stable ssAβ 1-42 strains for a genetic screen. A single integrated genomic copy of ssAβ 1-42 (1 x ssAβ 1-42) was not toxic, but the integration of multiple copies of the construct resulted in robust toxicity. (D) Aβ 1-42 expression in the vector control, the 1 x ssAβ, and two ssAβ screening strains was detected by immunoblot analysis using the 6E10 Aβ-specific antibody. Samples were loaded onto a Bis-Tris gel with and without prior boiling in LDS sample buffer. We detected higher molecular weight species of Aβ corresponding to trimers, tetramers and higher molecular weight oligomeric species only in the unboiled Aβ 1-42 samples, indicating that these species are indeed non-covalent oligomeric assemblies of Aβ. Asterisks (*) refer to non-specific reactivity of the antibody, as these proteins are also present in the vector control lysate. (E) Mass spectrometry of immunoprecipitated material from one of the Aβ screening strains. Extracts of a vector control and a ssAβ 1-42

screening strain were immunoprecipitated with the 6E10 antibody and this material was subjected to SDS-PAGE and silver staining. The ~3.5 kDa and 6 kDa region of each the control lane and the Aβ screening strain lane were excised. Proteins and peptides in these slices were eluted from the gel, subjected to tryptic digestion, and subjected to mass spectrometric analysis. The sequence of the human Aβ 1-42 peptide is shown and the sequence regions that are underlined are the sequences of the two tryptic peptides detected only in the ssAβ cells by mass spectrometry (HDSGYEVHHQK and LVFFAEDVGSNK). No other peptides were detected in either strain. (F) Lysate of ssAβ 1-42 screening strain 2 was fractionated using size exclusion chromatography. Individual fractions collected from the size exclusion column were individually assayed using an indirect ELISA assay with a monoclonal Aβ oligomer-specific antibody (referred to as OMAB). Molecular weights corresponding to fractions 7, 10, 12, 14 and 19 were calculated based on protein standards run on the same column using identical conditions. Data are representative of three independent experiments and shown as mean +/- SEM. (G) Aβ 1-40 and Aβ 1-42 expression was detected by immunoblot analysis of boiled lysates using 6E10.

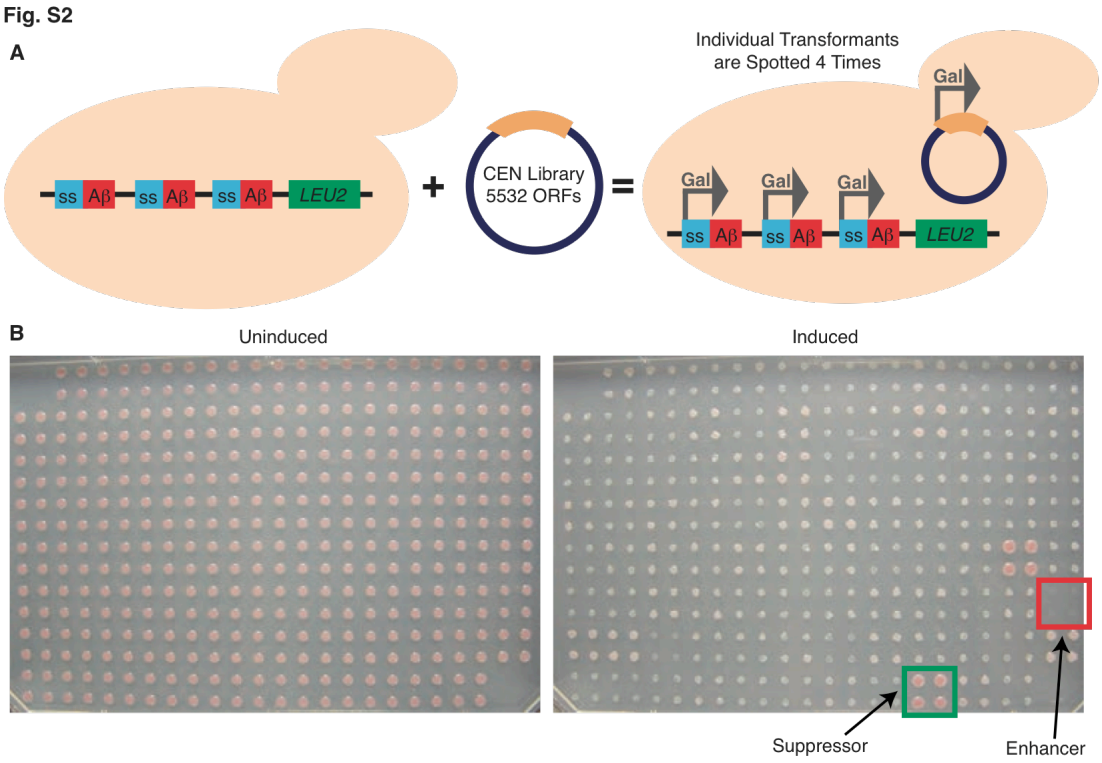

Fig. S2: Example of a screening plate
(A) Yeast strains carrying the ssAβ 1-42 construct and the Gal4-Estrogen Receptor (ER)-VP16 transcription factor were transformed with a CEN plasmid library containing a genome-wide collection of ORFs. (B) Each transformant was spotted 4 times in a square array using a Singer RoToR robot on media containing galactose, glucose and estradiol, glycerol and estradiol, or glucose alone as a non-inducing growth control. Enhancers resulted in decreased growth and suppressors in increased growth; refer to boxed examples. Empty quadrants on the plate are the result of empty wells in the plasmid library.

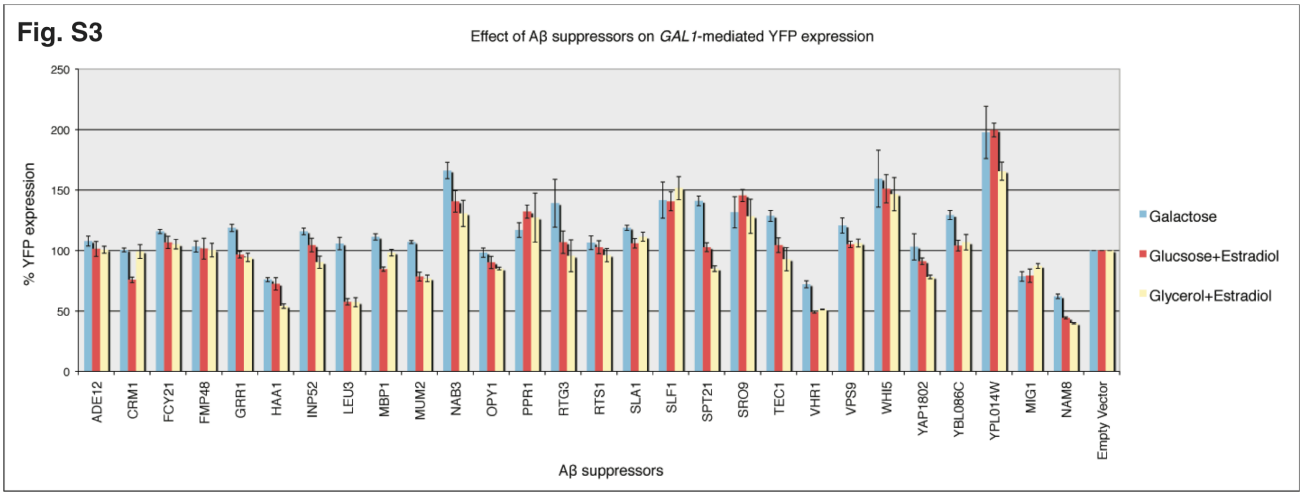

Fig. S3: Effect of suppressors on YFP expression levels
Putative suppressors may decrease Aβ toxicity by decreasing GAL1-mediated expression. We assessed whether any of the identified suppressors affected GAL1-mediated expression by assaying the expression of Yellow Fluorescent Protein (YFP) under the control of a GAL1 promoter. Putative suppressors were transformed into a strain carrying an integrated GAL1-controlled YFP construct and the Gal4-ER-VP16 transcription factor. The effect of putative hits on YFP expression levels was quantified using flow cytometry after overnight growth in one of three media conditions: galactose, glucose with estradiol or glycerol with estradiol. Hits that significantly decreased the levels of YFP in comparison to the vector control were eliminated as false positives (i.e. HAA1, LEU3 and VHR1). We did not eliminate suppressors that showed activity on all three media conditions, even if YFP expression levels were lower for one of the growth conditions.

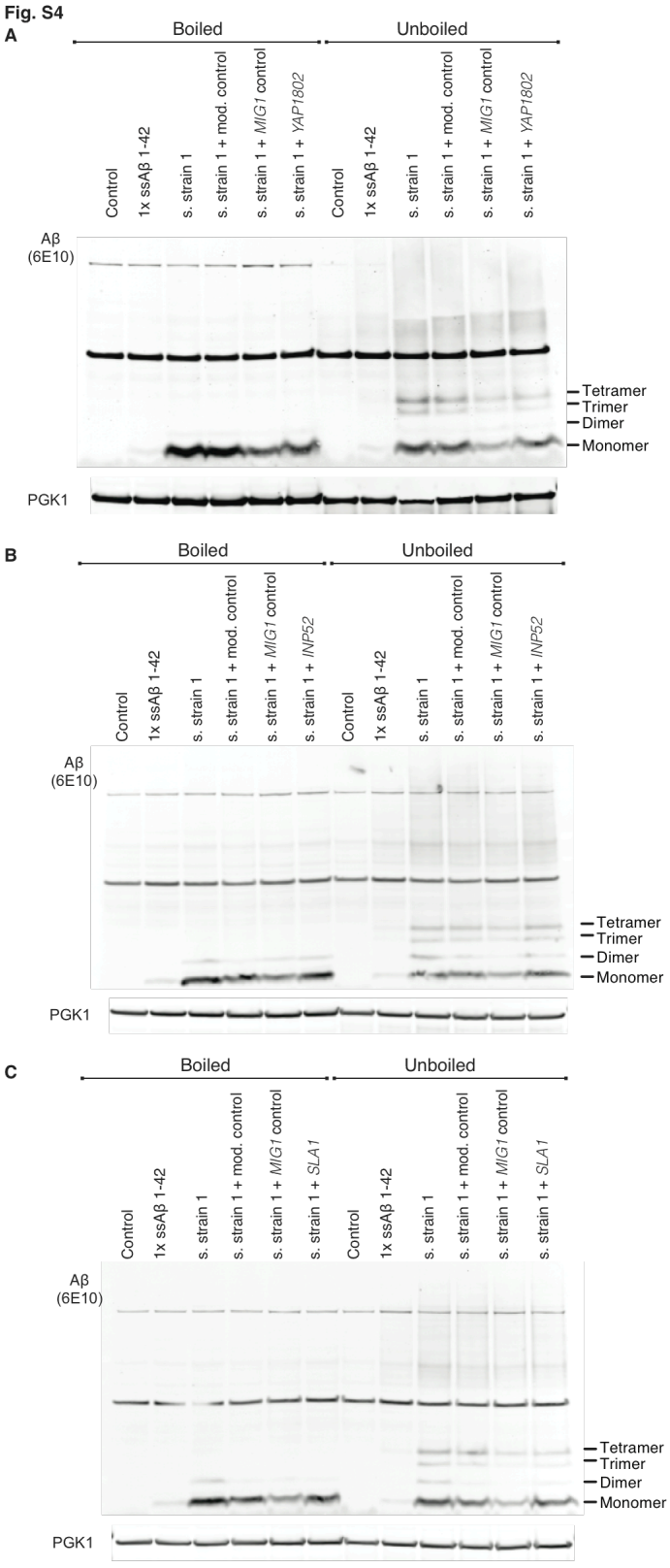

Fig. S4: Effect of *YAP1802, INP52,* and *SLA1* on Aβ levels.
We transformed the ssAβ 1-42 screening strain 1 with either a vector control plasmid, *MIG1* (control), or one of the following suppressors: (A) *YAP1802,* (B)

INP52, or (C) *SLA1*. The levels of Aβ 1-42 in each of these strains were assessed by immunoblot analysis with the 6E10 antibody. As expected, *MIG1*, which suppresses *GAL1*-mediated transcription, decreased levels of Aβ 1-42 expression, as compared to the vector control. The yeast expressing either (A) *YAP1802*, (B) *INP52,* or (C) *SLA1* showed a small decrease in the amount of low molecular weight oligomers as compared to the modifier vector control. The overall amount of Aβ 1-42 in the yeast expressing (A) *YAP1802*, (B) *INP52,* or (C) *SLA1* are remarkably similar to the level observed in the control lanes (refer to the boiled samples). These data suggest that these three modifiers induce only subtle changes in Aβ levels.

Fig. S5

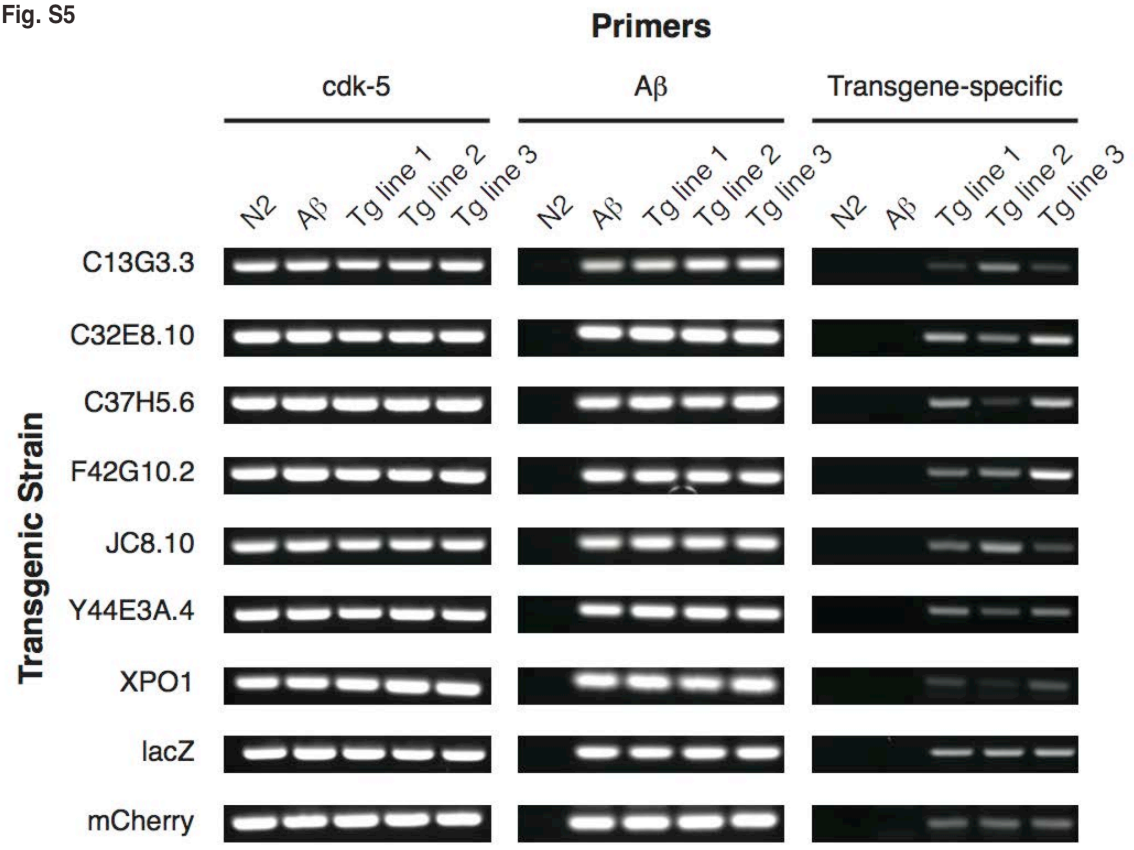

Fig. S5: Analysis of transgene expression in worm strains.
We conducted semi-quantitative RT-PCR to ensure that transgenes did not influence ssAβ 1-42 expression in *C. elegans*. We could not measure Aβ levels by western blot analysis as we expressed Aβ only in the glutamatergic neurons of the worms. The PCR was conducted by using primers designed to amplify *cdk-5* (control), Aβ, and indicated transgenic modifiers of Aβ-induced neurodegeneration. For all primers, a N2 wild-type strain served as both positive (*cdk-5*) and negative (Aβ and transgenes) controls. The ssAβ transgene of the Aβ strain (UA166) was integrated into worm chromosomal DNA to maintain steady Aβ expression levels in the entire organism (see Materials and Methods). Using UA166 strain, 9 additional transgenic strains expressing homologs of Aβ toxicity modifiers identified in the yeast genetic screen were generated. Expression levels of the corresponding modifiers varied since the transgenes remained as extrachromosomal arrays. To address the discrepancies, we generated 3 independent lines for each of the 9 transgenic strains. Importantly, co-expression of the modifiers did not change the ssAβ expression level.

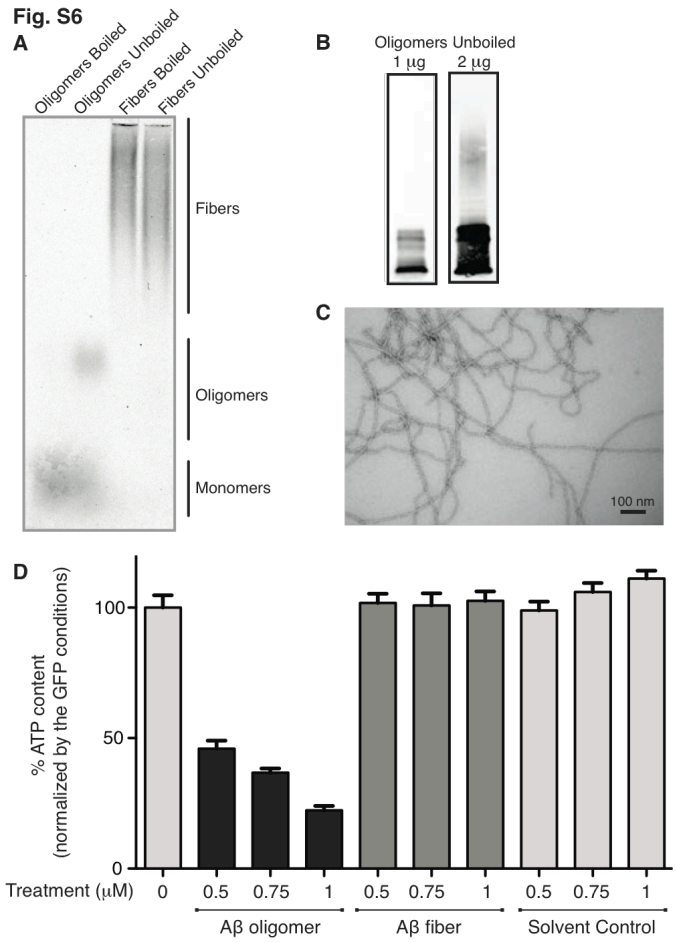

Fig. S6: Characterization of Aβ oligomers and Aβ fibers used in cortical neuron experiments.

(A) SDD-AGE characterization of Aβ 1-42 oligomers and Aβ 1-42 fibers prepared from synthetic peptide (see Materials and Methods). Oligomer and fiber samples were either not boiled or boiled in 6% sarkosyl buffer. These samples were subsequently run on a 1.2% SDD-AGE gel. Upon boiling, Aβ 1-42 oligomers collapsed into monomeric species, while unboiled oligomers ran as species of intermediate size on the SDD-AGE gel. Fiber samples were resistant to boiling, consistent with the formation of an SDS-resistant amyloid structure. (B) Unboiled Aβ 1-42 oligomers were also characterized by western blot using the 6E10 antibody. These samples contained a diversity of low and high molecular weight oligomeric species. (C) Aβ fiber formation was also detected by negative stain Electron Microscopy (EM). The scale bar is representative of 100 nm. (D) Cortical neuron cultures prepared from rat embryos at embryonic day 18 were cultured for 5 days, and were subsequently incubated for 20 hrs with either soluble Aβ oligomers or Aβ fibers prepared from synthetic peptide. Cell viability was assessed using ATP content. Data are representative of three independent experiments and shown as mean +/- SEM. Aβ fibers were not toxic to the cortical neurons, validating that toxicity to these neuronal cultures is mediated by the oligomeric nature of the Aβ 1-42 peptide.

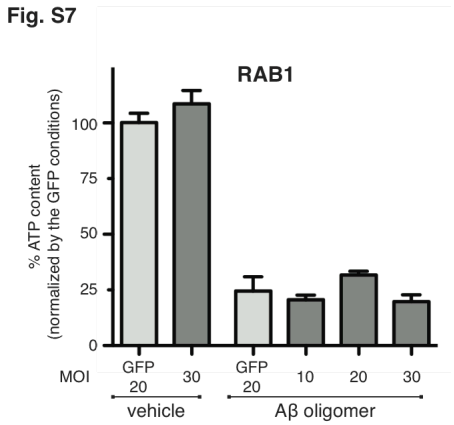

Fig. S7: *RAB1* does not rescue Aβ-induced toxicity in cortical neurons.
Cortical neuron cultures prepared from rat embryos at embryonic day 18 were cultured for 5 days, transduced, cultured for 13 days, and then incubated for 20 hrs with 750nM of soluble Aβ oligomers prepared from synthetic peptide. Infection with a *RAB1* lentiviral construct, a suppressor of neuronal α-syn toxicity, had no significant effect on Aβ oligomer toxicity. Cell viability was assessed by ATP content. Data are representative of three independent experiments and shown as mean +/- SEM (*: $P<0.05$; **: $P<0.01$, based on Dunnett's test).

Table S1. Propidium Iodide staining of strains expressing Aβ

We used propidium iodide (PI) staining to measure yeast cell death in our control strains and our strains expressing ssAβ 1-42. Of the 5000 cells counted for each sample, the % of cells dead (positive for PI) are indicated in the table above. These results show that there is no significant cell death caused by the expression of ssAβ 1-42 after 16 hrs of growth in galactose.

	% of Total Cells Dead
Control: No PI	0.1
Control: Dead Cells	99.76
Control: p305 Vector	8.56
1 x ssAβ 1-42	21.08
ssAβ 1-42 s. strain 1	12.62
ssAβ 1-42 s. strain 2	18.72

Table S2. Suppressors and enhancers of Aβ toxicity identified in the yeast screen

We constructed yeast strains with an intermediate level of Aβ expression and corresponding toxicity that allowed us to identify in the same screen genes that alleviated or enhanced toxicity when overexpressed (see Materials and Methods). Aβ toxicity is likely to be influenced by mitochondrial function in neurons (*55, 56*). We took advantage of the fact that the extent to which yeast rely on mitochondrial respiration is carbon source dependent, thereby allowing us to test the full library of ORFs at different levels of respiration. In glucose, cells ferment and respiration remains low until all glucose is converted to ethanol. In galactose respiration is moderately active. In glycerol, cells are completely dependent on respiration for growth. To determine if the effect of putative modifiers on Aβ toxicity depended on the level of mitochondrial respiration, we conducted our screen on the three different carbon sources mentioned: glucose, galactose and glycerol. The expression of both ssAβ 1-42 and the library of yeast ORFs were under control of the *GAL1* promoter. To induce expression in glucose and glycerol, we employed a chimeric Gal4-ER-VP16 transcription factor that enables induction of the *GAL1* promoter through the addition of the estrogen estradiol (*44*). We plated the ssAβ strains carrying two plasmids, the Gal4-ER-VP16 transcription factor on one and individual yeast ORFs on the other, on media containing galactose, glucose + estradiol, or glycerol + estradiol. We also plated cells on glucose alone as a non-inducing growth control.

Suppressors increased growth relative to a vector control on the indicated conditions; enhancers decreased it (see Fig. S2B for an example of a screening plate). The function and localization of the gene products identified as modifiers are based on Saccharomyces Genome Database (SGD) gene summaries.

Only a few of the modifiers, specifically *SLA1, RTG3, NAB3, SLF1, FCY21, VPS9, GRR1, YBL086c, IVY1, PBS2, PKC1* and *MVP1,* were strongly affected by the state of mitochondrial respiration. However, the fact that most of the suppressors and enhancers were reproduced on all three media indicates the robustness of their affects on Aβ toxicity.

Galactose	Glucose + Estradiol	Glycerol + Estradiol	Category	Systematic Name	Gene Name	Description	Human Homolog (HomoloGene prediction)	Human Homolog (pBlast)	Blast p-value
Suppressor	Suppressor	Suppressor	biosynthetic process	YNL220W	ADE12	Adenylosuccinate synthase, catalyzes the first step in synthesis of adenosine monophosphate from inosine 5'monophosphate during purine nucleotide biosynthesis.	ADSSL1	ADSSL1	3.00E-146
Suppressor	Suppressor	Suppressor	DNA replication	YBR057C	MUM2	Cytoplasmic protein essential for meiotic DNA replication and sporulation; interacts with Orc2p, which is a component of the origin recognition complex.			
Suppressor	Suppressor	Suppressor	endocytosis	YGR241C	YAP1802	Protein involved in clathrin cage assembly; binds Pan1p and clathrin; homologous to Yap1801p, member of the AP180 protein family.	PICALM	PiCALM	4.00E-26
-	Suppressor	Suppressor	endocytosis	YBL007C	SLA1	Cytoskeletal protein binding protein required for assembly of the cortical actin cytoskeleton; interacts with proteins regulating actin dynamics and proteins required for endocytosis; found in the nucleus and cell cortex; has 3 SH3 domains.	SH3KBP1 (functional homolog)	SH3RF3	6.00E-07
Suppressor	Suppressor	Suppressor	endocytosis	YNL106C	INP52	Polyphosphatidylinositol phosphatase, dephosphorylates a number of phosphatidylinositols (PIs) to PI; involved in endocytosis; hyperosmotic stress causes translocation to actin patches; synaptojanin-like protein with a Sac1 domain.	SYNJ1	SYNJ1	4.00E-125
Enhancer	Enhancer	Enhancer	endocytosis	YPL032C	SVL3	Protein of unknown function, mutant phenotype suggests a potential role in vacuolar function; green fluorescent protein (GFP)-fusion protein localizes to the cell periphery, cytoplasm, bud, and bud neck.			
Suppressor	Suppressor	Suppressor	kinase	YGR052W	FMP48	Putative protein of unknown function; the authentic, non-tagged protein is detected in highly purified mitochondria in high-throughput studies; induced by treatment with 8-methoxypsoralen and UVA irradiation.		MARK4	3.00E-21
Enhancer	Enhancer	Enhancer	kinase	YAL017W	PSK1	One of two PAS domain containing S/T protein kinases; coordinately regulates protein synthesis and carbohydrate metabolism and storage in response to a unknown metabolite that reflects nutritional status.		PASK	3.00E-50
Enhancer	-	Enhancer	kinase	YJL128C	PBS2	MAP kinase kinase that plays a pivotal role in the osmosensing signal-transduction pathway, activated under severe osmotic stress.	MAP2K4	MAP2K2	8.00E-69
Enhancer	Enhancer	-	kinase	YBL105C	PKC1	Protein serine/threonine kinase essential for cell wall remodeling during growth; localized to sites of polarized growth and the mother-daughter bud neck; homolog of the alpha, beta, and gamma isoforms of mammalian protein kinase C (PKC).		PKN2	5.00E-98
Enhancer	Enhancer	Enhancer	mannosyltransferase	YAL023C	PMT2	Protein O-mannosyltransferase, transfers mannose residues from dolichyl phosphate-D-mannose to protein serine/threonine residues; acts in a complex with Pmt1p, can instead interact with Pmt5p in some conditions; target for new antifungals.	POMT2	POMT2	6.00E-124
Enhancer	Enhancer	Enhancer	nuclear migration	YPL269W	KAR9	Karyogamy protein required for correct positioning of the mitotic spindle and for orienting cytoplasmic microtubules, localizes at the shmoo tip in mating cells and at the tip of the growing bud in small-budded cells through anaphase.			
Suppressor	Suppressor	Suppressor	protein transport	YGR218W	CRM1	Major karyopherin, involved in export of proteins, RNAs, and ribosomal subunits from the nucleus; exportin.	XPO1	XPO1	0.00E+00
Enhancer	Enhancer	Enhancer	response to mercury ion	YNL042W	BOP3	Protein of unknown function, potential Cdc28p substrate; overproduction confers resistance to methylmercury.			
Enhancer	Enhancer	Enhancer	RNA processing	YGL173C	KEM1	Evolutionarily-conserved 5'-3' exonuclease component of cytoplasmic processing (P) bodies involved in mRNA decay; plays a role in microtubule-mediated processes, filamentous growth, ribosomal RNA maturation, and telomere maintenance.	XRN1	XRN1	0.00E+00
Suppressor	Suppressor		signal transduction	YOR014W	RTS1	B-type regulatory subunit of protein phosphatase 2A (PP2A); homolog of the mammalian B' subunit of PP2A.	PPP2R5C	PPP2R5C	3.00E-153
Enhancer	Enhancer	Enhancer	signal transduction	YAL009W	SPO7	Putative regulatory subunit of Nem1p-Spo7p phosphatase holoenzyme, regulates nuclear growth by controlling phospholipid biosynthesis, required for normal nuclear envelope morphology, premeiotic replication, and sporulation.			
Enhancer	Enhancer	Enhancer	signal transduction	YGR070W	ROM1	GDP/GTP exchange protein (GEP) for Rho1p; mutations are synthetically lethal with mutations in Rom2, which also encodes a GEP.		NET1	5.00E-14
Enhancer	Enhancer	Enhancer	signal transduction	YLR332W	MID2	O-glycosylated plasma membrane protein that acts as a sensor for cell wall integrity signaling and activates the pathway; interacts with Rom2p, a guanine nucleotide exchange factor for Rho1p.			
Enhancer	Enhancer	Enhancer	signal transduction	YBL061C	SKT5	Activator of Chs3p (chitin synthase III), recruits Chs3p to the bud neck via interaction with Bni4p.		SEL1L2	9.00E-10
Suppressor	Suppressor	Suppressor	transcription factor	YOR083W	WHI5	Repressor of G1 transcription that binds to SCB binding factor (SBF) at SCB target promoters in early G1; phosphorylation of Whi5p by the CDK, Cln3p/Cdc28p relieves repression and promoter binding by Whi5.			
Suppressor	Suppressor	Suppressor	transcription factor	YLR014C	PPR1	Zinc finger transcription factor containing a Zn(2)-Cys(6) binuclear cluster domain, positively regulates transcription of genes involved in uracil biosynthesis.			
Suppressor	Suppressor	Suppressor	transcription factor	YBR083W	TEC1	Transcription factor required for full Ty1 expression, Ty1-mediated gene activation, and haploid invasive and diploid pseudohyphal growth; TEA/ATTS DNA-binding domain family member.		TEAD2	1.00E-10
-	Suppressor	Suppressor	transcription factor	YBL103C	RTG3	Basic helix-loop-helix-leucine zipper (bHLH/Zip) transcription factor that forms a complex with another bHLH/Zip protein, Rtg1p, to activate the retrograde (RTG) and TOR pathways.		MITF	6.00E-09
Suppressor	Suppressor	Suppressor	transcription factor	YDL056W	MBP1	Transcription factor involved in regulation of cell cycle progression from G1 to S phase, forms a complex with Swi6p that binds to MluI cell cycle box regulatory element in promoters of DNA synthesis genes.		DAPK1	1.00E-08
Enhancer	Enhancer	Enhancer	transcription factor	YIL122W	POG1	Putative transcriptional activator that promotes recovery from pheromone induced arrest; inhibits both alpha-factor induced G1 arrest and repression of CLN1 and CLN2 via SCB/MCB promoter elements; potential Cdc28p substrate; SBF regulated.			
Suppressor	Suppressor	Suppressor	transcription regulation	YMR179W	SPT21	Protein with a role in transcriptional silencing; required for normal transcription at several loci including HTA2-HTB2 and HHF2-HHT2, but not required at the other histone loci.			
-	Suppressor	Suppressor	transcription regulation	YPL190C	NAB3	Single stranded RNA binding protein; acidic ribonucleoprotein; required for termination of non-poly(A) transcripts and efficient splicing.			
-	Suppressor	Suppressor	translation regulation	YDR515W	SLF1	involved in the copper-dependent mineralization of copper sulfide complexes on cell surface in cells cultured in copper salts.		LARP1	4.00E-08
Suppressor	Suppressor	Suppressor	translation regulation	YCL037C	SRO9	Cytoplasmic RNA-binding protein that associates with translating ribosomes; involved in heme regulation of Hap1p as a component of the HMC complex, also involved in the organization of actin filaments; contains a La motif.		LARP1B	3.00E-12
Enhancer		Enhancer	translation regulation	YMR257C	PET111	Mitochondrial translational activator specific for the COX2 mRNA; located in the mitochondrial inner membrane.			

Enhancer	Enhancer	Enhancer	translation regulation	YLR139C	SLS1	Mitochondrial membrane protein that coordinates expression of mitochondrially-encoded genes; may facilitate delivery of mRNA to membrane-bound translation machinery.			
-	-	Suppressor	transport	YER060W	FCY21	Putative purine-cytosine permease.			
Enhancer	Suppressor	Suppressor	transport	YJR090C	GRR1	F-box protein component of the SCF ubiquitin-ligase complex; involved in carbon catabolite repression, glucose-dependent divalent cation transport, high-affinity glucose transport, morphogenesis, and sulfite detoxification.	FBXL2	FBXL20	4.00E-24
-	Suppressor	Suppressor	transport	YML097C	VPS9	A guanine nucleotide exchange factor involved in vesicle-mediated vacuolar protein transport; specifically stimulates the intrinsic guanine nucleotide exchange activity of Vps21p/Rab5: similar to mammalian ras inhibitors; binds ubiquitin.	RABGEF1	RABGEF1	4.00E-24
-	Suppressor	Suppressor	unknown	YBL086C	YBL086C	Protein of unknown function; green fluorescent protein (GFP)-fusion protein localizes to the cell periphery.			
Suppressor	Suppressor	Suppressor	unknown	YPL014W	YPL014W	Putative protein of unknown function; green fluorescent protein (GFP)-fusion protein localizes to the cytoplasm and to the nucleus.			
Suppressor	Suppressor	Suppressor	unknown	YBR129C	OPY1	Protein of unknown function, overproduction blocks cell cycle arrest in the presence of mating pheromone; the authentic, non-tagged protein is detected in highly purified mitochondria in high-throughput studies.			
-	Enhancer	Enhancer	vacuole	YDR229W	IVY1	Phospholipid-binding protein that interacts with both Ypt7p and Vps33p, may partially counteract the action of Vps33p and vice versa, localizes to the rim of the vacuole as cells approach stationary phase.			
Enhancer	Enhancer	-	vacuole	YMR004W	MVP1	Protein required for sorting proteins to the vacuole; overproduction of Mvp1p suppresses several dominant VPS1 mutations; Mvp1p and Vps1p act in concert to promote membrane traffic to the vacuole.	SNX8	SNX8	6.00E-21

Table S3. Genome-wide FBAT-GEE association results from NIMH coh

To test for support for a genetic association between AD and our eleven candidate genes we revisited the family-based genome-wide association screen (GWAS) analysis (*31*) performed on the National Institute of Mental Health (NIMH) Genetics Alzheimer's Disease Initiative Study (*32*). The sample consisted of 1,217 participants from 439 families of self-reported European ancestry. Genotyping was prepared with the GeneChip Human Mapping 500K Array Set from Affymetrix. Within the eleven gene regions, plus a 50-kb window proximally and distally, 133 SNPs passed quality control assessment (using PLINK v1.07) and were tested for association using a family-based association test (FBAT v3.6) approach.

The FBAT method is similar in design to a classic transmission disequilibrium test method in which the genotype distribution in the affected is compared to its expected distribution under the null hypothesis. To optimize statistical power, age of onset and AD affection status were tested together as a combined outcome variable, by use of the multivariate extension of the FBAT-approach, FBAT-GEE (Generalized Estimating Equation). We assumed an additive genetic model to test for association between our outcome variable and genotype.

Table S3 contains a subset of tested SNPs from the genome-wide FBAT-GEE association analysis that was pruned based on linkage disequilibrium. Pruning was performed with the "indep" command in PLINK which reduces a set of SNPs into a subset that are in approximate linkage equilibrium with each other. Selection of the subset is based on the variance inflation factor 1/(1-R2), R2 is the multiple correlation coefficient for a SNP being regressed on all other SNPs concurrently. Additional features of the pruning are described on the PLINK website under the LD-base SNP pruning sections.

The association for the XPO1 SNP rs6545886 is robust to a Bonferroni adjustment for the 4 independent SNPs tested at each locus (P_{adj}=0.003 * 4 = 0.012).

Gene	SNP	Chr.	Position[1]	MAF[2]	Fams[3]	FBAT-GEE[4]
PICALM	rs10501603	11	85,359,564	0.23	172	0.03
PICALM	rs615887	11	85,367,689	0.24	159	0.01
PICALM	rs597446	11	85,452,707	0.39	215	0.03
PICALM	rs568755	11	85,483,910	0.32	193	0.04
PICALM	rs659023	11	85,502,507	0.35	206	0.29
PPP2R5	rs11625483	14	101,321,490	0.38	206	0.86
PPP2R5	rs1746598	14	101,333,217	0.08	77	0.72
PPP2R5	rs8016207	14	101,366,968	0.18	149	0.98
PPP2R5	rs8015021	14	101,379,446	0.08	63	0.21
PPP2R5	rs10873529	14	101,481,601	0.28	179	0.14
ADSSL1	rs4983386	14	104,281,252	0.46	239	0.29

XPO1	rs7563678	2	61,653,462	0.4	216	0.17
XPO1	rs778755	2	61,692,688	0.45	216	0.07
XPO1	rs17010833	2	61,714,960	0.05	48	0.42
XPO1	rs6545886	2	61,733,522	0.11	109	0.003
SYNJ1	rs845022	21	32,920,977	0.42	187	0.61
SYNJ1	rs845006	21	32,953,727	0.06	60	0.68
SYNJ1	rs928754	21	33,006,701	0.48	195	0.6
FBXL20	rs755500	17	34,663,391	0.26	175	0.09
RABGEF1	rs12537474	7	65,749,172	0.08	136	0.64
XRN1	rs1552340	3	143,498,288	0.42	225	0.33
POMT2	rs8009261	14	76,810,128	0.44	210	0.56
POMT2	rs3783986	14	76,832,625	0.4	203	0.59
POMT2	rs1861889	14	76,833,554	0.08	72	0.66
POMT2	rs4899651	14	76,854,215	0.25	178	0.29
SNX8	rs7805462	7	2,122,849	0.32	192	0.62
MAP2K4	rs1468501	17	11,862,669	0.26	184	0.75
MAP2K4	rs976244	17	11,897,717	0.21	171	0.93
MAP2K4	rs9907196	17	11,925,064	0.2	167	0.98
MAP2K4	rs4791490	17	11,989,069	0.19	145	0.16
MAP2K4	rs7208899	17	12,075,716	0.06	54	0.94

[1]Physical position from Build 27 NCBI36/Hg18
[2]Minor allele frequency (MAF)
[3]Number of informative families from FBAT-GEE analysis
[4]*P*-value from family-based association test (FBAT)

Table S4. Cohort demographics and characteristics

Clinical, pathological and genotype data from the Religious Orders Study and Rush Memory and Aging Project were used to clinically validate significance of our screen results. Age indicates the time of last evaluation for the clinical cohort, and time of death for the pathology cohort. AD clinical diagnosis was based on NINCDS criteria, inclusive of probable and possible AD.

	Clinical	**Pathological**
N	1593	651
age[1]	85	87.9
female (%)	69.4	62.4
AD[2] **(%)**	22.1	40.9

[1]Age at last evaluation (clinical) or death (pathological)

[2]Clinical diagnosis of Alzheimer's disease based on NINCDS criteria (probable or possible)

Table S5. Human loci tested for associations with intermediate AD cognitive and neuropathologic phenotypes.

We comprehensively evaluated both genotyped and imputed common variation at human homologs for 11 out of 12 of the top results of our yeast screen. We were unable to evaluate the human functional homolog of Sla1, *SH3KBP1*, due to imprecise imputation on the X chromosome. At each locus, all SNPs from the quality-controlled, genome-wide genotyping dataset were extracted from RefSeq-based genomic coordinates, inclusive of a 50-kb genomic window, both proximal and distal. The size of each locus analyzed and the resultant number of SNPs tested is shown.

YEAST GENE	HUMAN HOMOLOG	Chr	Hg18 Coordinates[1]	Size (kb)	SNPs tested (n)
YAP1802	*PICALM*	11	85296132 - 85507756	211	187
RTS1	*PPP2R5C*	14	101295924 - 101513830	218	144
ADE12	*ADSSL1*	14	104211578 - 104334692	123	42
CRM1	*XPO1*	2	61508572 - 61668922	160	45
INP52	*SYNJ1*	21	32872943 - 33072148	199	109
GRR1	*FBXL20*	17	34620365 - 34861402	241	80
VPS9	*RABGEF1*	7	65793077 - 65963883	171	78
KEM1	*XRN1*	3	143458138 - 143699543	241	66
PMT2	*POMT2*	14	76761051 - 76906970	146	148
MVP1	*SNX8*	7	2211164 - 2370625	160	67
PBS2	*MAP2K4*	17	11814859 - 12037776	223	114

[1]Based on RefSeq gene consensus, plus a 50-kb window both proximally and distally.

Table S6. Locus associations with episodic memory decline.

Using PLINK software, each locus-based SNP set was evaluated for associations with rate-of-change in episodic memory performance within the combined ROS and MAP clinical cohort, based on repeated assessments of 7 neuropsychiatric tests. Linear regression analyses were adjusted for baseline age, gender, and years of education. For each locus, this analysis defines the strongest, independent marker SNP. For each such SNP, the minor/reference allele (A1), allele frequency (Frq), effect size (Beta & 95% CI), as well as *P*-value (*P*) are shown. In order to determine if the observed locus association is significance, a permutation test was performed, in which phenotype labels were permuted 1000 times, in order to determine an empirical *P*-value (P_{perm}), adjusting for the number of SNPs tested at each locus. The results was considered significant for P_{perm}<0.05 (bold); whereas P_{perm}<0.1 was interpreted as suggestive (asterisk). Of the 11 loci evaluated, *PICALM* was found to be associated with decline in episodic memory performance, and several additional loci showed suggestive association signals.

YEAST GENE	HUMAN HOMOLOG	best SNP[1]	A1[2]	Frq	Beta (95% CI)	*P*	P_{perm}[3]
YAP1802	*PICALM*	rs7128598	G	0.25	-0.016 (-0.025 to -0.008)	1.59E-04	**0.012**
RTS1	*PPP2R5C*	rs10873529	G	0.27	0.009 (0.001 to 0.017)	0.029	0.614
ADE12	*ADSSL1*	rs11851852	T	0.03	-0.033 (-0.055 to -0.011)	0.003	0.072*
CRM1	*XPO1*	rs967968	C	0.47	0.010 (0.003 to 0.017)	0.007	0.079*
INP52	*SYNJ1*	rs13339977	T	0.02	0.026 (0.001 to 0.052)	0.045	0.559
GRR1	*FBXL20*	rs11657409	T	0.27	-0.009 (-0.018 to 0.0004)	0.062	0.476
VPS9	*RABGEF1*	rs13224487	G	0.01	0.045 (0.012 to 0.077)	0.007	0.076*
KEM1	*XRN1*	rs6440083	G	0.29	0.011 (0.003 to 0.019)	0.005	0.062*
PMT2	*POMT2*	rs2042045	A	0.34	-0.010 (-0.018 to -0.003)	0.009	0.299
MVP1	*SNX8*	rs4721548	G	0.44	-0.006 (-0.014 to 0.001)	0.086	0.816
PBS2	*MAP2K4*	rs7221795	A	0.08	-0.017 (-0.030 to -0.004)	0.012	0.230

[1]Strongest SNP association observed at each locus.

[2]minor/reference allele

[3]Empirically-determined *P*-value from permutation test. Significant results (*P*<0.05) boldfaced; Suggestive results (*P*<0.1) asterisked.

Table S7. Locus associations with global AD pathology

Using PLINK software, each locus-based SNP set was evaluated for associations with a quantitative measure of global AD pathology within the combined ROS and MAP autopsy cohort, based on averaged counts of neuritic plaques, diffuse plaques, and neurofibrillary tangles from 5 brain regions. Linear regression analyses were adjusted for age at the time of death. For each locus, this analysis defines the strongest, independent marker SNP. For each such SNP, the minor/reference allele (A1), allele frequency (Frq), effect size (Beta & 95% CI), as well as *P*-value (*P*) are shown. In order to determine if the observed locus association is significance, a permutation test was performed, in which phenotype labels were permuted 1000 times, in order to determine an empirical *P*-value (P_{perm}), adjusting for the number of SNPs tested at each locus. The results was considered significant for P_{perm}<0.05 (bold). *ADSSL1* and *RABGEF1* were each found to harbor significant signals of association with the global AD pathology measure.

YEAST GENE	HUMAN HOMOLOG	best SNP[1]	A1[2]	Frq	Beta (95% CI)	*P*	P_{perm}[3]
YAP1802	*PICALM*	rs7950477	T	0.02	0.219 (0.068 to 0.371)	0.005	0.157
RTS1	*PPP2R5C*	rs6575881	T	0.005	-0.364 (-0.680 to -0.048)	0.024	0.548
ADE12	*ADSSL1*	rs1128880	G	0.48	0.098 (0.039 to 0.156)	0.001	**0.031**
CRM1	*XPO1*	rs2518934	C	0.44	-0.042 (-0.085 to 0.0002)	0.052	0.357
INP52	*SYNJ1*	rs7284048	A	0.08	0.056 (-0.024 to 0.137)	0.172	0.951
GRR1	*FBXL20*	rs16968748	G	0.02	-0.165 (-0.335 to 0.006)	0.059	0.513
VPS9	*RABGEF1*	rs17566701	T	0.48	-0.067 (-0.111 to -0.024)	0.002	**0.038**
KEM1	*XRN1*	rs13101141	A	0.06	-0.045 (-0.137 to 0.046)	0.331	0.970
PMT2	*POMT2*	rs2287385	A	0.16	0.077 (0.021 to 0.133)	0.007	0.244
MVP1	*SNX8*	rs3807428	A	0.05	-0.095 (-0.190 to -0.001)	0.048	0.630
PBS2	*MAP2K4*	rs12603093	C	0.25	0.040 (-0.009 to 0.089)	0.107	0.916

[1]Strongest SNP association observed at each locus.

[2]minor/reference allele

[3]Empirically-determined *P*-value from permutation test. Significant results (*P*<0.05) boldfaced; Suggestive results (*P*<0.1) asterisked.

Additional References

43. S. Alberti, A. D. Gitler, S. Lindquist, A suite of Gateway cloning vectors for high-throughput genetic analysis in Saccharomyces cerevisiae. *Yeast* **24**, 913 (2007).
44. M. J. Quintero, D. Maya, M. Arevalo-Rodriguez, A. Cebolla, S. Chavez, An improved system for estradiol-dependent regulation of gene expression in yeast. *Microb Cell Fact* **6**, 10 (2007).
45. R. Halfmann, S. Lindquist, Screening for amyloid aggregation by Semi-Denaturing Detergent-Agarose Gel Electrophoresis. *J Vis Exp*, (2008).
46. R. Howson *et al.*, Construction, verification and experimental use of two epitope-tagged collections of budding yeast strains. *Comp Funct Genomics* **6**, 2 (2005).
47. P. Lamesch *et al.*, C. elegans ORFeome version 3.1: increasing the coverage of ORFeome resources with improved gene predictions. *Genome Res* **14**, 2064 (2004).
48. P. Lamesch *et al.*, hORFeome v3.1: a resource of human open reading frames representing over 10,000 human genes. *Genomics* **89**, 307 (2007).
49. S. Brenner, The genetics of Caenorhabditis elegans. *Genetics* **77**, 71 (1974).
50. J. A. Lewis, J. T. Fleming, Basic culture methods. *Methods Cell Biol* **48**, 3 (1995).
51. S. Hamamichi *et al.*, Hypothesis-based RNAi screening identifies neuroprotective genes in a Parkinson's disease model. *Proc Natl Acad Sci U S A* **105**, 728 (2008).
52. C. Lesuisse, L. J. Martin, Long-term culture of mouse cortical neurons as a model for neuronal development, aging, and death. *J Neurobiol* **51**, 9 (2002).
53. L. B. Chibnik *et al.*, CR1 is associated with amyloid plaque burden and age-related cognitive decline. *Ann Neurol*, (2010).
54. K. Frazer *et al.*, A second generation human haplotype map of over 3.1 million SNPs. *Nature* **449**, 851 (2007).
55. G. E. Gibson, Q. Shi, A mitocentric view of Alzheimer's disease suggests multi-faceted treatments. *J Alzheimers Dis* **20 Suppl 2**, S591 (2010).
56. J. X. Chen, S. S. Yan, Role of mitochondrial amyloid-beta in Alzheimer's disease. *J Alzheimers Dis* **20 Suppl 2**, S569 (2010).